https://doi.org/10.5194/egusphere-2024-1707
Preprint. Discussion started: 12 June 2024

Reconstruction of Holocene and Last Interglacial vegetation dynamics and wildfire activity in southern Siberia

Jade Margerum[1], Julia Homann[2], Stuart Umbo[1], Gernot Nehrke[3], Thorsten Hoffmann[2], Anton Vaks[4], Aleksandr Kononov[5,6], Alexander Osintsev[7], Alena Giesche[8], Andrew Mason[9], Franziska A. Lechleitner[10], Gideon M. Henderson[9], Ola Kwiecien[1], Sebastian F.M. Breitenbach[1]

[1] Department of Earth and Environmental Sciences, Northumbria University, Newcastle-Upon-Tyne, NE1 8ST, United Kingdom
[2] Department Chemie, Johannes Gutenberg-Universität Mainz, Duesbergweg 10-14, 55128 Mainz, Germany
[3] Alfred Wegener Institut Helmholtz-Zentrum für Polar- und Meeresforschung, Section Marine BioGeoSciences, 27570 Bremerhaven, Germany
[4] Geological Survey of Israel, 32 Yeshayahu Leibowitz Street, 9692100 Jerusalem, Israel
[5] Irkutsk Nation al Research Technical University, Irkutsk, 664074, Russia
[6] Institute of the Earth's Crust, Russian Academy of Sciences, Siberian Branch, Irkutsk, 664033, Russia
[7] Speleoclub Arabika, St. Mamina-Sibiryaka 6a, 664058 Irkutsk, Russia
[8] U.S. Geological Survey, Alaska Science Center, Anchorage, Alaska 99508, USA
[9] Department of Earth Sciences, University of Oxford, South Parks Road, OX1 3AN Oxford, UK
[10] Department of Chemistry, Biochemistry and Pharmaceutical Sciences & Oeschger Centre for Climate Change Research, Universität Bern, Freiestrasse 3, 3012 Bern, Switzerland

Correspondence to: Jade Margerum (jade.margerum@northumbria.ac.uk)

Key words. Stalagmites, Lignin oxidation products, Levoglucosan, Paleoenvironments

Abstract. Wildfires are a rapidly increasing threat to boreal forests. While our understanding of the drivers behind wildfires and their environmental impact is growing, it is mostly limited to the observational period. Here we focus on the boreal forests of southern Siberia, and exploit a U-Th dated stalagmite from Botovskaya cave (55.2994°N, 105.4445°E), located in the upper Lena region of southern Siberia, to document wildfire activity and vegetation dynamics during parts of two warm periods; the last interglacial (124.1 – 118.8 ka BP) and the Holocene (10 – 0 ka BP). Our record is based on levoglucosan (Lev), a biomarker sensitive to biomass burning, and on lignin oxidation products (LOPs) that discriminate between open and closed forest and hard- or softwood vegetation. In addition, we used carbon stable isotope ratios ($\delta^{13}C$) to evaluate soil respiration and local infiltration changes. While the $\delta^{13}C$ record reflects a dominant control of the host rock, the Lev and LOP time series show fire pattern and vegetation type differences between the last interglacial and the Holocene. Our LOP data suggest that during the last interglacial, the region around Botovskaya cave was characterised by open forest, which by ca. 121.5 ka BP underwent a transition from fire-resistant hardwood to fire-prone softwood. The Lev record indicates that fire activity was high and increased towards the end of last interglacial just before 119 ka BP. In contrast, the Holocene was characterised by a closed-forest environment with mixed hard- and softwood vegetation. Holocene fire activity varied but at a much lower level than

https://doi.org/10.5194/egusphere-2024-1707
Preprint. Discussion started: 12 June 2024

during the last interglacial. We attribute the changes in wildfire activity during the intervals of interest to the interplay between vegetation and climate. The open forests of the last interglacial were more likely to ignite than their closed Holocene equivalents, and their flammability was aided by warmer and drier summers and a stronger seasonal temperature contrast compared to the Holocene. Our comparison of the last two interglacial intervals suggests that with increasing global temperatures the boreal forest of southern Siberia becomes progressively more vulnerable to higher wildfire activity.

1. Introduction

Ongoing global warming results in (pan)regional changes in hydrological and temperature seasonality (Brunello et al., 2019; Swain, 2021), cryosphere extent (Kamp et al., 2022; Schuur et al., 2022) and the composition of the global biosphere (Steffen et al., 2018), which collectively affects the recurrence and intensity of droughts (Laaha et al., 2016) and wildfires (Schuur et al., 2022; Westerling et al., 2006). Global changes in vegetation and wildfire have far-reaching consequences, including further deterioration of biodiversity, and result in a positive feedback loop between fires, vegetation vulnerability, and climate change (Bowman et al., 2020; Cochrane and Bowman, 2021; Senande-Rivera et al., 2022). The combined effects of global warming and land-use change increase the flammability of many landscapes worldwide (Bowman et al., 2020), but the future magnitude and environmental consequences of wildfires at regional-to-local scales remain unclear. Siberia, hosting permafrost and boreal forest, two recently redefined climate tipping elements (McKay et al., 2022), is a region that is highly vulnerable to rising temperature–wildfire positive feedback. Fire activity in Siberia is highest between April and September, and is influenced by competing meteorological conditions such as temperature, precipitation, humidity, wind speed, as well as land cover type, fuel availability (vegetation), and stand structure (tree species size and distribution) (Forkel et al., 2012; Tomshin and Solovyev, 2022).

According to global climate model projections, the fire-prone area of all boreal zones is likely to increase by the end of the 21st century (Senande-Rivera et al., 2022). Boreal forests of the Northern Hemisphere already show a trend to more frequent and intense wildfires (Kharuk et al., 2021, 2023; Walker et al., 2019). In the southern Siberian boreal forest belt, mean annual air temperatures have increased at twice the rate of the global terrestrial average, and have accelerated since the early 1990s, driving the increase in forest fires (Balzter et al., 2007; Lugina et al., 2006; Talucci et al., 2022). The powerful Siberian heatwaves in 2010, 2020, and 2021 led to aggravated wildfire activity that has been linked to anthropogenic climate change (Ciavarella et al., 2021; Hantemirov et al., 2022).

Increased wildfire activity has been identified as a potential driver of intensified permafrost thaw (Ciavarella et al., 2021; Talucci et al., 2022), and slowed forest recovery after burning (Ponomarev et al., 2016; Sun et al., 2021). Higher frequency of wildfires could transform boreal forests from carbon sinks to sources (Brazhnik et al., 2017; Dolman et al., 2012; Masyagina

https://doi.org/10.5194/egusphere-2024-1707
Preprint. Discussion started: 12 June 2024

& Menyailo, 2020). Therefore, understanding the future of wildfires and their causes and effects demands an approach that integrates monitoring of recent occurrences (collecting metrics data like fire seasonality, intensity, severity, and area) with insights from paleo-fire research (particularly focused on past thermal maxima with conditions similar to those expected over the coming decades). Currently, our knowledge of palaeo-wildfire behaviour in the Siberian boreal ecosystem is limited to northern regions based on reconstructions from ice cores (Eichler et al., 2011), and charcoal, black carbon, and anhydrites records in lake surface sediments (Dietze et al., 2020; Glückler et al., 2021, 2022), which identify climate, wildfire activity, and vegetation type back to ca. 430 ka BP. In southern Siberia, observational data (e.g., remote sensing data of burned area) (García-Lázaro et al., 2018) are available only since the early 2000s (Bondur et al., 2023; García-Lázaro et al., 2018), and the only study that explores wildfire and vegetation changes in the past is limited to the Holocene (Barhoumi et al., 2021).

Speleothems (i.e., secondary cave carbonate deposits, like stalagmites and flowstones) offer a large array of environmentally sensitive proxies (i.e., stable isotopes and trace elements) that inform on past hydrological, environmental, and climatic changes. Levoglucosan (Lev) is a monosaccharide biomarker that is solely produced through the combustion of cellulose at temperatures between 150-350°C (Simoneit et al., 1999) and has been widely applied as a proxy for wildfire activity in various paleoclimatic archives, like ice cores and lake sediments (Segato et al., 2021; Zennaro et al., 2014). Lev has recently been utilised in speleothems (Homann et al., 2022, 2023), where, as a compound, it remains stable and protected from erosion or degradation over long time periods.

Lignins are naturally occurring biopolymers that are found in terrestrial vascular plants (Jex et al., 2014), and are well-preserved during transport from soil to cave and within speleothem carbonate (Heidke et al., 2018). Lignin oxidation products (LOPs) are categorised as cinnamyl (C), syringyl (S), and vanillyl (V), and the S/V and C/V ratios delineate different vegetation types such as woody vs. non-woody and hardwoods vs. softwoods (Jex et al., 2014). Consequently, the combination of Lev and LOPs from the same archive can provide insights into frequency of local wildfires and the type of vegetation (fuel) that was burning.

We present a wildfire and vegetation reconstruction for southern Siberia outside the Lake Baikal macroclimate zone for both the Holocene and the second half of the last interglacial (LIG). Comparing our record with regional reconstructions places past fire activity in a wider environmental framework. Finally, we evaluate the relationship between wildfire activity and vegetation type during these two interglacial periods, comparing and contrasting Holocene and last interglacial conditions from a perspective of recent warming.

https://doi.org/10.5194/egusphere-2024-1707
Preprint. Discussion started: 12 June 2024

1.1 Study site

Botovskaya cave (55.2994°N, 105.4445°E) is in southern Siberia, Russia, 250 km NW of Lake Baikal (Fig. 1). The cave is located atop a south-facing slope at 750 m above sea level (for details, see supplemental data in Vaks et al. 2013, 2020). The overlying bedrock geology is comprised of Ordovician (488.3 – 443.7 Ma) limestone and sandstone. The cave is 20 – 40 m below the surface and consists of a myriad of (sub)horizontal passages created by phreatic widening of tectonic faults and fractures, of which >70 km have been mapped (Appendix A, Fig. A1). The mean cave air temperature was monitored between 2010 and 2018 and fluctuates between 1.6 and 1.9°C in warmer areas and stays just above 0°C in colder areas of the cave (Appendix B Fig. B1) (Vaks et al., 2013, 2020). Today, speleothems grow actively only in a few areas and inactive speleothem formations are widespread and often broken through frost action.

Our study region is characterised by a continental climate, with short, cool summers and severe, dry winters (Dwc climate in the Köppen-Geiger classification; Peel et al., 2007). Regional atmospheric circulation and climate in southern Siberia are influenced by the Atlantic westerlies that bring moisture eastwards, and the Siberian High that dominates atmospheric circulation between autumn and spring and facilitates dry conditions by blocking moisture derived from the westerlies (Kostrova et al., 2020). During summer, the Siberian High weakens and is replaced by the Asiatic low, and warm and unstable air masses cause heavy rainstorms between July and August. Mean monthly summer and winter temperatures at the nearby Zhigalovo meteorological station (55 km south of Botovskaya cave), recorded between the late 1930s to 1990s, were 15.3 ± 1.2 °C and -26 ± 3.6 °C respectively, but in recent years (2000 – 2019), mean monthly summer temperatures have increased >1 °C to 16.7 ± 1.2 °C and winter temperatures by nearly 2 °C to -24.2 ± 3.9 °C. Local air temperatures recorded just outside the entrance to Botovskaya cave were higher compared to the Zhigalovo meteorological station that is located in the Lena river valley where frequent temperature inversions result in colder mean air temperatures than at the higher-altitude Botovskaya cave. The mean annual precipitation is 345 mm/a of which 55 % falls between June and August.

https://doi.org/10.5194/egusphere-2024-1707
Preprint. Discussion started: 12 June 2024

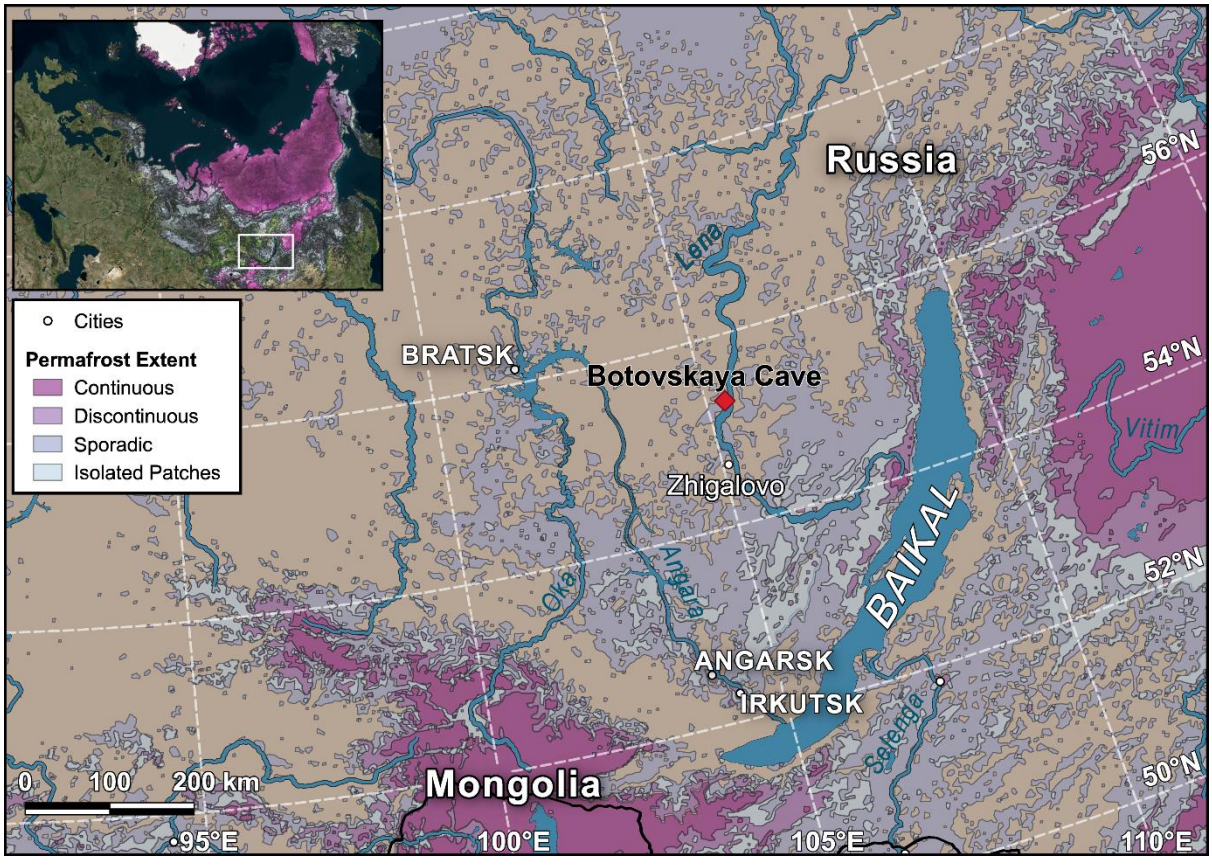

Figure 1: Location of Botovskaya cave in southern Siberia, Russia. Permafrost zones within our study area are derived from modelled permafrost probabilities (Obu et al., 2019). Botovskaya cave is within the zone of sporadic permafrost.

125 The plateau above the cave is characterized by a sub-boreal closed-canopy taiga forest, consisting of both gymnosperm (softwood) and angiosperm (hardwood) trees. Softwood species include larch (*Larix sibirica)*, fir (*Abies sibirica)*, Siberian cedar pine (*Pinus sibirica)*, and Scots pine (*Pinus sylvestris)*, while hardwood species include birch (*Betula* spp.*)*, aspen (*Populus tremula)*, and cherry (*Prunus* spp.). The understory is represented by shrub species such as redcurrant (*Ribes rubrum*) and blackcurrant (*Ribes nigrum*), as well as mosses, lichen, and liverwort (Ponomarev et al., 2016).

130

https://doi.org/10.5194/egusphere-2024-1707
Preprint. Discussion started: 12 June 2024

2. Material and Methods

2.1 Sample description and minerology

Sample SB_pk7497-1, a 11 cm long stalagmite (Fig. 2), was found broken in a hydrologically active location ca. 1.1 km from the central entrance of Botovskaya cave (see Appendix A, Fig. 1A). The sample was sliced along the growth axis to provide two halves, one of which was used to perform all measurements required for this study. A macroscopically discernible detrital layer at 71.5 mm from the top of the sample marks a hiatus. It is possible that the SB_pk7497-1 record extended back further, however the sample was found broken, and we were unable to locate the older segment in the cave. This specimen has been utilised in previous studies to investigate past permafrost (Vaks et al., 2013) and carbon cycle dynamics (Lechleitner et al., 2020).

Mineral species calcite and aragonite were identified at the Alfred Wegener Institute Helmholtz-Zentrum for Polar and Marine Research, Germany, using confocal Raman microspectrometry to map the growth axis. Thirteen Raman spectra were measured using an excitation wavelength of ~480 nm, a spectrometer grating of 1800 g/mm, 500 nm blaze, and an integration time of 0.05 s. The obtained maps each measured ca. 17.5 mm by 4 mm and were used for correction of stable isotope data (see 3.5).

2.2 Radiometric dating

Seven U-Th dates were milled with a 1 mm tungsten carbide drill bit and measured at the University of Oxford, UK. The dates have been previously published in (Vaks et al. 2013, 2020). Contamination was minimised by milling and discarding the top ca. 50 µm of the sample surface before milling the powder for analysis. The U-Th dates and hiatus location and proxy data were input into the COPRA software routine (Breitenbach et al., 2012) to construct an age-depth model along the speleothem growth axis.

2.3 Levoglucosan and Lignin sample preparation

Forty subsamples of 500 ± 80 mg were milled at ca. 3 mm resolution from SB-pk7497-1 at Northumbria University, UK, for levoglucosan and lignin analyses. Twenty subsamples originated from above the hiatus and 20 from below. All subsequent sample preparation and analyses were completed at Johannes Gutenberg-University Mainz, Germany.

Levoglucosan and LOP analyses were conducted following the methodology described by Homann et al. (2022). In short, the pulverised samples were spiked with $^{13}C_6$ levoglucosan, extracted with methanol, and evaporated in salinated vials. The evaporated residue was redissolved and filtered to 0.2 µm. The remaining sample carbonate was dried and dissolved in hydrochloric acid and polymeric lignin was extracted using solid phase extraction (SPE). Because of the large samples required for lignin analysis it was necessary to combine adjacent samples used in levoglucosan analysis (i.e., 1-2, 3-4, 5-6, etc.). Lignin

https://doi.org/10.5194/egusphere-2024-1707
Preprint. Discussion started: 12 June 2024

samples were subjected to an oxidative digestion and the resultant LOPs extracted from solution with another SPE. Solutions were filtered to 0.2 µm prior to analysis.

Levoglucosan and LOP analyses were conducted on a Dionex UltiMate 3000 ultra high-performance liquid chromatography system coupled to a heated electrospray ionisation source and Q Exactive Orbitrap high resolution mass spectrometer.

2.4 Stable isotopes

Subsamples for stable oxygen and carbon isotopes were taken at 1 mm resolution across the central growth axis of SB_pk7497-1. Of a total of 116 samples taken, 73 were above and 43 below the hiatus. Carbonate powders of 30-60 µg were measured on a Thermo Fisher Scientific Delta V Plus mass spectrometer, coupled to a ConFlo IV and a ThermoFinnigan Gasbench II at ETH Zurich, following the methodology of Breitenbach & Bernasconi (2011) and (Spötl, 2004). All isotope values were calibrated against Vienna Pee-Dee Belemnite (VPDB) and reported in delta notation. Analytical uncertainties were < 0.06 ‰ (1σ) for $\delta^{13}C$ and < 0.08 ‰ (1σ) for $\delta^{18}O$. Because calcite and aragonite, or a mixture of both, are observed in the stalagmite, isotope results were corrected using the Raman maps. All results were corrected for their predominant minerology using the fractionation factors and methods proposed in Fohlmeister et al. (2018).

3. Results

3.1 Stalagmite fabric and minerology

Stalagmite minerology was identified by Raman mapping as predominantly aragonite, with frequent transitions between both calcite and aragonite especially in the lower half (Fig. 2). Occasionally, there are regions where mineral composition is uniformly distributed within the growth layer.

3.2 Radiometric dating and age-depth model

SB_pk7497-1 yielded five dates analogous with the Holocene, and two LIG dates (Fig. 2). These dates do not cover the entirety of the Holocene (0 – 11.7 ka BP) or LIG (115 – 130 ka BP), but rather intervals within these periods, specifically between 0 – 10 ka BP and 118.8 – 124.1 ka BP. From here, when referring to the Holocene and LIG (unless stated otherwise), these terms will refer to the intervals covered by our proxy timeseries as indicated above. The high U content (36 – 158 ppm) in this stalagmite yielded low age uncertainties of ≤ 50 years for the Holocene (younger than 9.87 ka BP) and < 320 years prior to 118.8 ka BP (last interglacial). Based on the COPRA model the stalagmite was actively growing from the middle LIG (124.1 ka BP) through the late LIG (118.8 ka BP) and resumed growth in the early Holocene (9.9 ka BP) until almost present day (0.3 ka BP). Mean Holocene growth rate was 8.4 µm/a whereas during the LIG it was higher at ~10 µm/a.

https://doi.org/10.5194/egusphere-2024-1707
Preprint. Discussion started: 12 June 2024

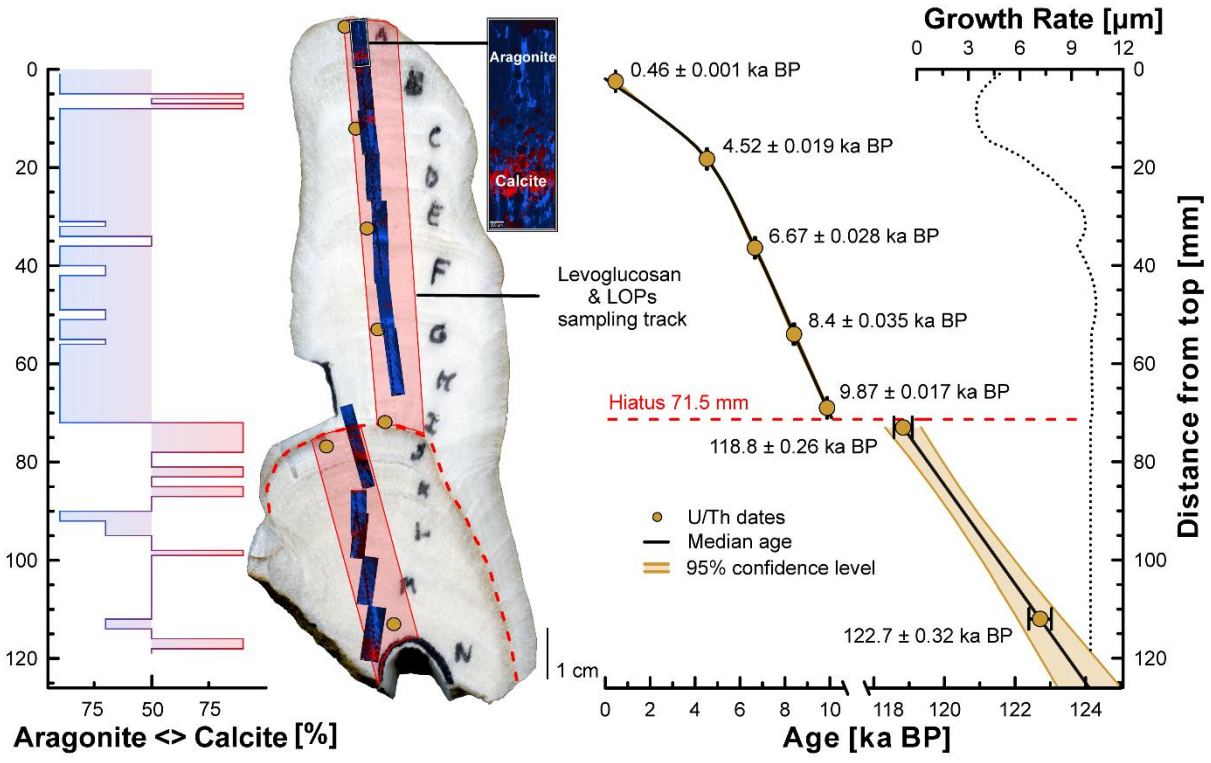

Figure 2: Distribution of U-Th dates and age uncertainties along stalagmite SB_pk7497-1. The COPRA median age model (black line) is constrained by 7 U-series dates (gold circles with 2s error bars). The hiatus is shown as dashed red line. The golden lines and shading highlight the 95% confidence bounds of the age-depth model. Growth rate varies from ca. 9.8 µm/a during the LIG and early Holocene to ca. 3.4 µm/a in the late Holocene (black dotted line). The red shaded area shows the sampling area for levoglucosan and lignin. Raman maps were taken along the growth axis and depict aragonite (blue) and calcite (red) sections (overlay on stalagmite scan).

3.3 Levoglucosan

Levoglucosan (Lev) sampling resolution of 93 ± 0.0002 years was achieved for the LIG, and of 139 ± 68 years for the Holocene (Fig. 3A) Lev concentrations range between 4.7 ng/g to 8.8 ng/g in the LIG, compared with 1.2 ng/g to 2 ng/g during the Holocene.

LIG Lev concentrations remain relatively stable between 124 – 121 ka BP. The lowest LIG concentration (5.2 ng/g) was measured in the interval corresponding to 121 – 119.5 ka BP. The end of our LIG record at 118.8 ka BP is marked by a near doubling in Lev concentration to 8.8 ng/g. This marks the highest Lev concentration measured in our stalagmite.

Holocene Lev concentrations are relatively stable and much lower compared to the LIG (Fig. 3A). The highest values of 2 ng/g occur in the early Holocene between 10 – 9 ka BP, followed by low amplitude changes around 1.5 ng/g. Lowest values are observed at 6.8, 5 and between 4 – 2 ka BP.

https://doi.org/10.5194/egusphere-2024-1707
Preprint. Discussion started: 12 June 2024

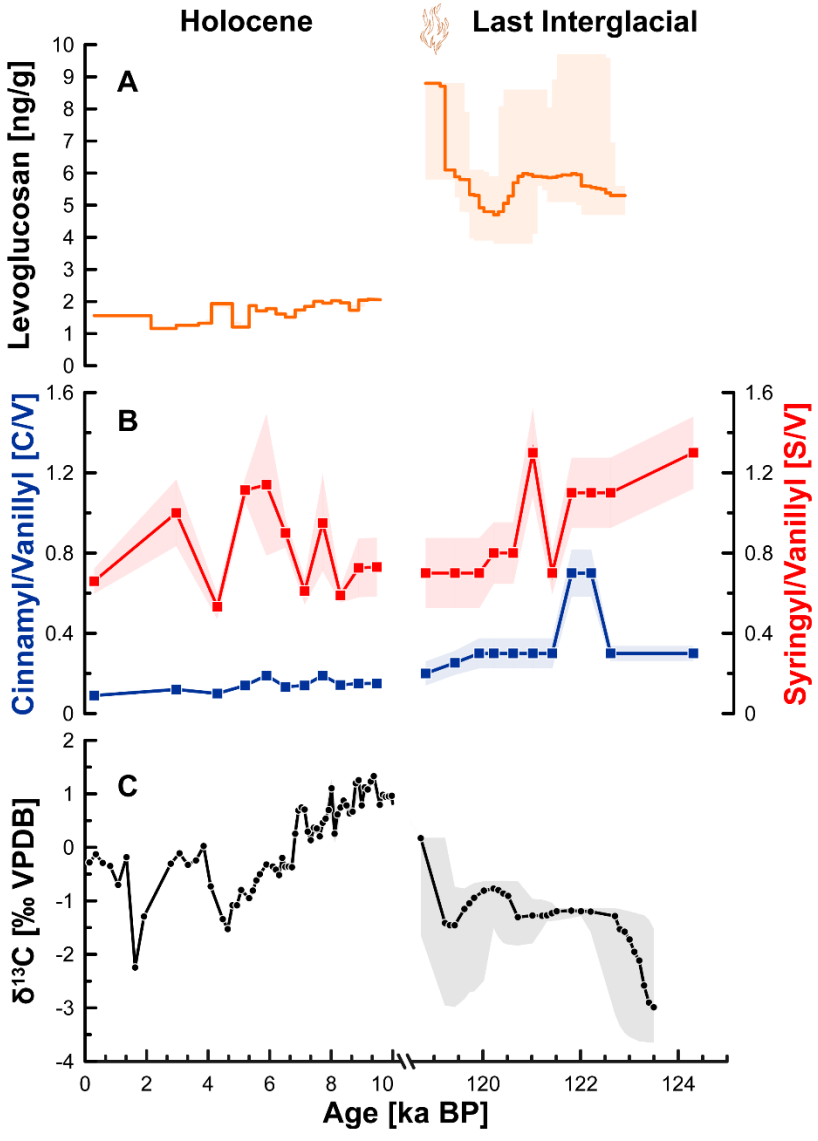

Figure 3: (A) Median levoglucosan concentration (orange line) with 95% confidence intervals (shaded area). (B) Median C/V (blue) and S/V (red) ratios with 1σ error margins (shaded area). (C) Median δ13C (black) with 95% confidence intervals (shaded area). Confidence intervals were derived from 2000 Monte Carlo simulations in the COPRA age modelling calculations and incorporate the interpolation and transfer of age uncertainty into the proxy domain. Error was negligible during the Holocene in plots A, B (CV) and C.

3.4 Lignin oxidation products (LOPs)

LOP sampling resolution of 920 ± 651 years was achieved for the LIG and 550 ± 410 years for the Holocene. Concentration ratios are based on phenolic structure of syringyl (S), cinnamyl (C), and vanillyl (V) (Fig. 3B and Table S4).

https://doi.org/10.5194/egusphere-2024-1707
Preprint. Discussion started: 12 June 2024

S/V ratios exhibit similar values (between 0.5 and 1.5) and variability in both the LIG and Holocene, in contrast to the C/V ratios which are generally higher (0.2 – 1.2) during the LIG compared to the Holocene (<0.2).

The LIG is characterised primarily by a gradual decrease in the S/V ratio, while the C/V ratio remains relatively constant, aside from a positive excursion between 122.5 and 122 ka BP. We find the lowest C/V and S/V ratios of the LIG at 119 ka, before our record is interrupted by the onset of glacial conditions. The late LIG S/V and C/V ratios are similar to those found in the early Holocene. Holocene C/V ratios remain stable whereas S/V ratios show high variability on millennial timescales. The lowest C/V ratios are measured in the youngest section of the record.

3.5 Stable isotopes

Across the LIG and the Holocene $\delta^{18}O$ varies between -17.2 and -12.8 ‰ and $\delta^{13}C$ varies between -3 and 1 ‰. Presently, the robust interpretation of $\delta^{18}O$ data is hindered by insufficient information from other moisture- and temperature-related proxies and here we discuss only vegetation-related $\delta^{13}C$ data. The LIG stable isotope record (Fig. 3C) broadly shows a 2 – 3 ‰ shift towards less negative values between 124 to 118.8 ka BP. During the early Holocene (until 5 ka BP), the $\delta^{13}C$ values show a long-term decrease overlaid by short-term variability. The late Holocene (after 5 ka BP) shows a shift to less negative values, punctuated by one excursion to lower values.

4. Discussion

The dominant vegetation type in the region surrounding a cave can be identified using the ratios of LOPs extracted from speleothems (Homann et al., 2022). In determining the vegetation type (softwood vs. hardwood, woody vs. non-woody) we follow the classification by Hedges & Mann (1979). Hardwood and softwood vegetation can be distinguished by elevated or reduced S/V ratios respectively (Fig. 4). High C/V ratios indicate woody plants while low C/V ratios reflect non-woody open vegetation. Hardwood vs. softwood and woody vs. non-woody plants differ in flammability and in recovery time after burning (Tepley et al., 2018), hence knowing the vegetation composition (fuel) is an important factor in understanding past wildfire dynamics. Furthermore, wildfire activity (i.e., temporal dynamics) can be revealed by levoglucosan (Lev) concentration in palaeoenvironmental timeseries. Levoglucosan and lignin proxy records from Siberian stalagmites offer new insights into interglacial vegetation composition and wildfire reoccurrence in understudied southern Siberia. Both vegetation composition and wildfire activity differ between the LIG and the Holocene, painting a picture of a sparsely forested and fire-prone environment during the LIG and a forested and fire-resilient environment during the Holocene. Our interpretation of the LOP, levoglucosan, and $\delta^{13}C$ records is supported by independent reconstructions of seasonal insolation (Laskar et al., 2004), Greenland air temperature (Andersen et al., 2004), and precipitation, temperature, and moisture estimates derived from Lake Baikal pollen profiles (Tarasov et al. 2005, 2007).

https://doi.org/10.5194/egusphere-2024-1707
Preprint. Discussion started: 12 June 2024

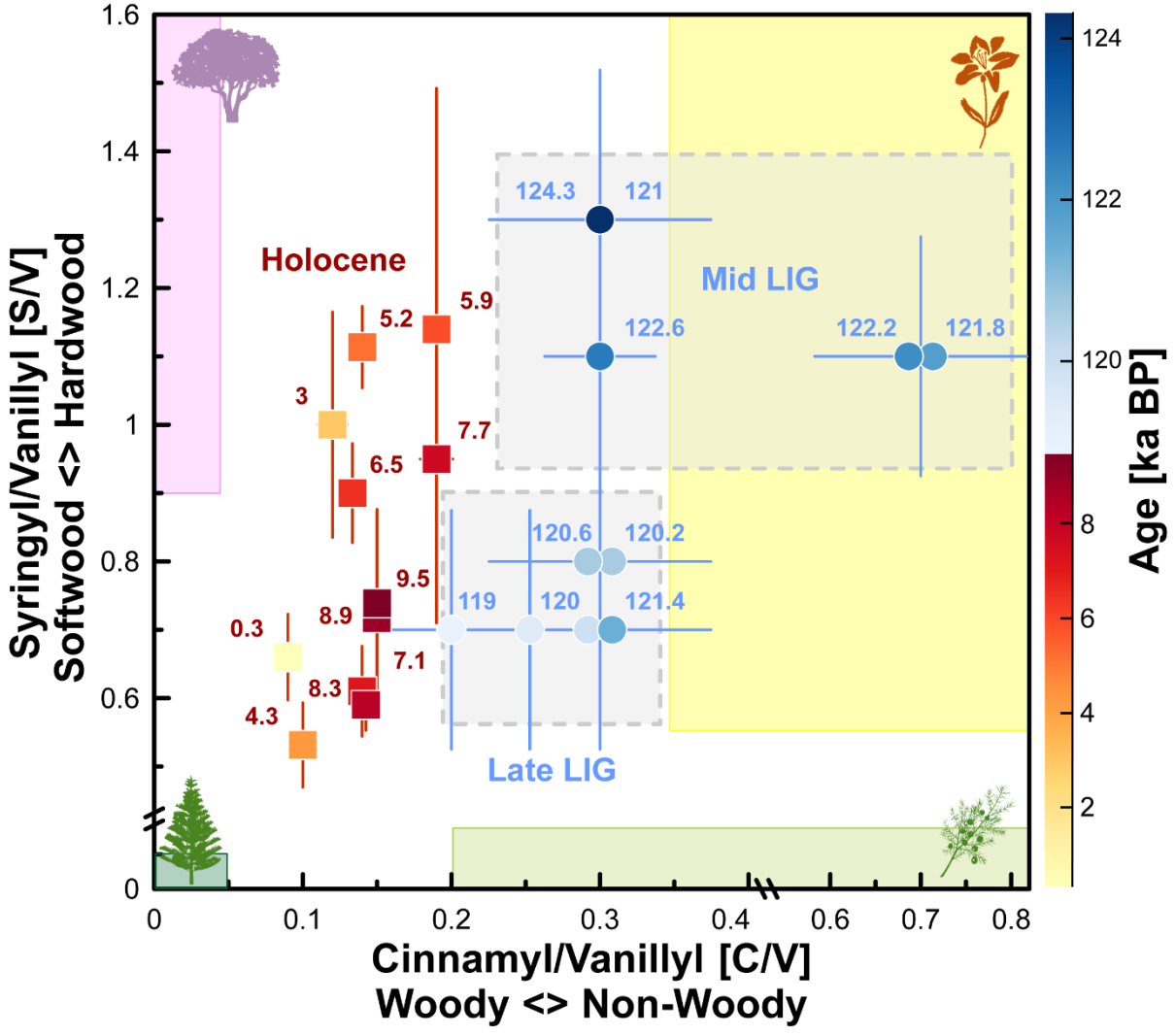

Figure 4: Stalagmite-based S/V vs. C/V ratios reflect changes in vegetation composition during the last interglacial (LIG) and the Holocene. Samples are color-coded by age, with darker colours indicative of older samples. Red points are Holocene samples and the blue LIG samples. Overlapping samples were adjusted left/right for clarity (e.g., 122.2 – 121.8 ka). The shaded boxes denote experimentally-determined LOP ratios of predominant species (Hedges and Mann, 1979); dark green is dominated by softwood woody plants, light-green by softwood non-woody plants, pink denotes hardwood woody plants, and yellow indicates hardwood non-woody plants. Mid-LIG and late LIG are highlighted by grey-shaded boxes. The Holocene is characterised by more woody vegetation compared to the LIG. Icons (pine tree, juniper bush, flower, and deciduous tree) are all sourced from www.freepick.com.

https://doi.org/10.5194/egusphere-2024-1707
Preprint. Discussion started: 12 June 2024

4.1 Last interglacial vegetation composition and wildfire activity

Relatively high C/V values point to dominance of non-woody taxa (steppe-like vegetation) during the mid LIG. High S/V values suggest that sparse woody taxa present were composed of hardwood species (e.g., birch and aspen) above Botovskaya cave – species which are normally restricted by the presence of permafrost (Kharuk et al., 2023). Lev concentrations are also high at that time and signify high wildfire activity (Fig. 5 B-C). According to a pollen-based quantitative reconstruction of LIG climate from Lake Baikal (Tarasov et al., 2007; Fig. 5 E-G), southern Siberian mean temperatures of the warmest and coldest months during the LIG were ca. 17°C and -22°C, respectively (vs. 15.3°C and -26°C today), whereas global maximum annual temperatures were ca. 2°C warmer than pre-industrial (Capron et al., 2014; Turney and Jones, 2010). The pollen data also indicate higher-than-present annual precipitation and moisture. We suggest that a warmer growth season in spring and summer (Fig. 5 E), high summer insolation (Fig. 5 H) and higher precipitation (Fig. 5 F) allowed hardwood species to advance northward and begin occupying larger areas previously dominated by softwood. Hardwood species are less flammable in low-intensity fires (Bryukhanov et al., 2018) and reproduce and mature faster than their softwood counterparts following burning (Shvetsov et al., 2019). These adaptions facilitate rapid post-fire recolonisation and regrowth, and constitute a competitive advantage over softwood species after burning (Belcher et al., 2021). Hardwood species such as birch have been observed to replace softwood species like larch in regular (80 – 120 years recurrence interval) wildfire activity scenarios (Shvetsov et al., 2019). The high S/V values at ca. 124 ka BP (Fig. 5 B) likely reflect similar replacement dynamics. A modern analogue for this scenario can be found in today's steppe and forest-steppe zones of southern Siberia, where high wildfire activity leads to expansion and succession of hardwood-dominated vegetation, with grasses, shrubs, and hardwood species quickly repopulating areas affected by wildfire and higher mortality of conifer seedlings (Kharuk et al., 2021; Tchebakova et al., 2009).

Declining C/V values and lower S/V values over the course of the later LIG (Fig. 5 A – B) document a transition from steppe-like vegetation towards more closed-canopy forests and from hardwood to softwood. This type of vegetation is more susceptible to wildfire, and the transition reflected in the LOP record is concomitant to an abrupt increase in Lev concentration that reflects increased wildfire activity at ca. 119.2 ka BP. Regional climate records indicate that the late LIG became cooler and drier, with lower annual precipitation and available moisture, and reduced surface temperatures (Tarasov et al., 2007; Fig. 5 E-G). The insolation curve points to increasing temperature seasonality with colder winters and warmer summers, while the Greenland ice core record suggests hemispheric cooling (Andersen et al., 2004; Fig. 5 H-I)). The cooling triggered a vegetation transition to more softwood-dominated forests that were better adapted to drier summers and harsh winters. Because this vegetation type is more vulnerable to wildfires, these conditions likely supported more frequent and intense wildfires. The decrease of regional surface temperatures (Fig. 5 E) ushered in the onset of the last glacial and eventually led to the return of continuous permafrost (which is indicated by the cessation of speleothem growth after ca. 118.8 ka BP).

https://doi.org/10.5194/egusphere-2024-1707
Preprint. Discussion started: 12 June 2024

During a short period between 122.2 and 121.8 ka BP within the LIG, higher C/V values suggest a transition from woody vegetation to non-woody (e.g., grasslands) (Fig. 5 A). This relatively short transition was likely a symptom of continuously high wildfire activity, as evidenced by increasing Lev concentrations. When forests burn frequently, higher fire-induced vegetation mortality can create patchy habitats leading to succession of pioneering non-woody vegetation and creating open spaces for grassland and meadows where forests usually stand. We suggest that this relatively short (ca. 400 year) period was a temporary transition when forests could not recover due to continuously high wildfire activity (in this case, likely higher *frequency*, as less-woody vegetation burns more readily under drier conditions). The return to pre-excursion C/V values by ca. 121.5 ka BP suggests that wildfires were not frequent enough to induce a permanent transition to a non-forested, open landscape.

An abrupt increase in Lev concentrations after 119 ka BP indicates significantly increased wildfire activity (Fig. 5 C). This could have been induced by drier and still warm summers in the late LIG that would have promoted dry lightning (the only natural ignition source for wildfires in Siberia), which considerably increases the probability of wildfires (Hessilt et al., 2022). Alongside softwood prevalence, this would have supported the expansion of fire into wider areas. The observed increase in wildfire activity in the late LIG was facilitated by natural processes and not by humans, which likely arrived in the Lena river valley only during the last glacial (Shichi et al., 2023; Weber et al., 2011).

The outlined vegetation and wildfire dynamics are supported by our stalagmite $\delta^{13}C$ record that reflects the interplay between open vs. forested vegetation (as indicated by the C/V values), temperature (Fig. 5 A-E), and soil respiration. A greater contribution of open vegetation (e.g., grasslands) during the LIG (Fig. 5 A) would result in less negative $\delta^{13}C$ values (Fig. 5 C). High summer temperatures dry out the topsoil and reduce soil respiration despite high precipitation events (thunderstorms), resulting in increasing $\delta^{13}C$ values (Fohlmeister et al., 2020). Increased drought stress in vegetation, as a result of higher temperatures, may add to the observed $\delta^{13}C$ trend (Fohlmeister et al., 2020). This is especially notable near the end of the LIG (118.8 ka BP) when, despite the prevalence of a more forested landscape (lower C/V ratios), high $\delta^{13}C$ values suggest that vegetation may have suffered from growth season drought and reduced productivity.

The LOP-based vegetation reconstruction for the LIG suggests an earlier transition from hardwood species to softwood species than regional reconstructions based on pollen data from Lake Baikal (e.g., Granoszewski et al., 2005; Tarasov et al. 2005, 2007). We observe a higher concentration of hardwood species during the mid LIG (from 124 to 121 ka BP), whereas pollen records (Granoszewski et al., 2005) indicate less hardwood developed in the Baikal region between 123.8 – 118.8 ka BP. We argue that our reconstruction from Botovskaya cave reflects relatively local vegetation dynamics that are separated from the Baikal Lake records by distance (250 km) and relatively high mountain ridges, while the lake record integrates a much larger catchment area that is more representative of general trends in southern Siberia.

https://doi.org/10.5194/egusphere-2024-1707
Preprint. Discussion started: 12 June 2024

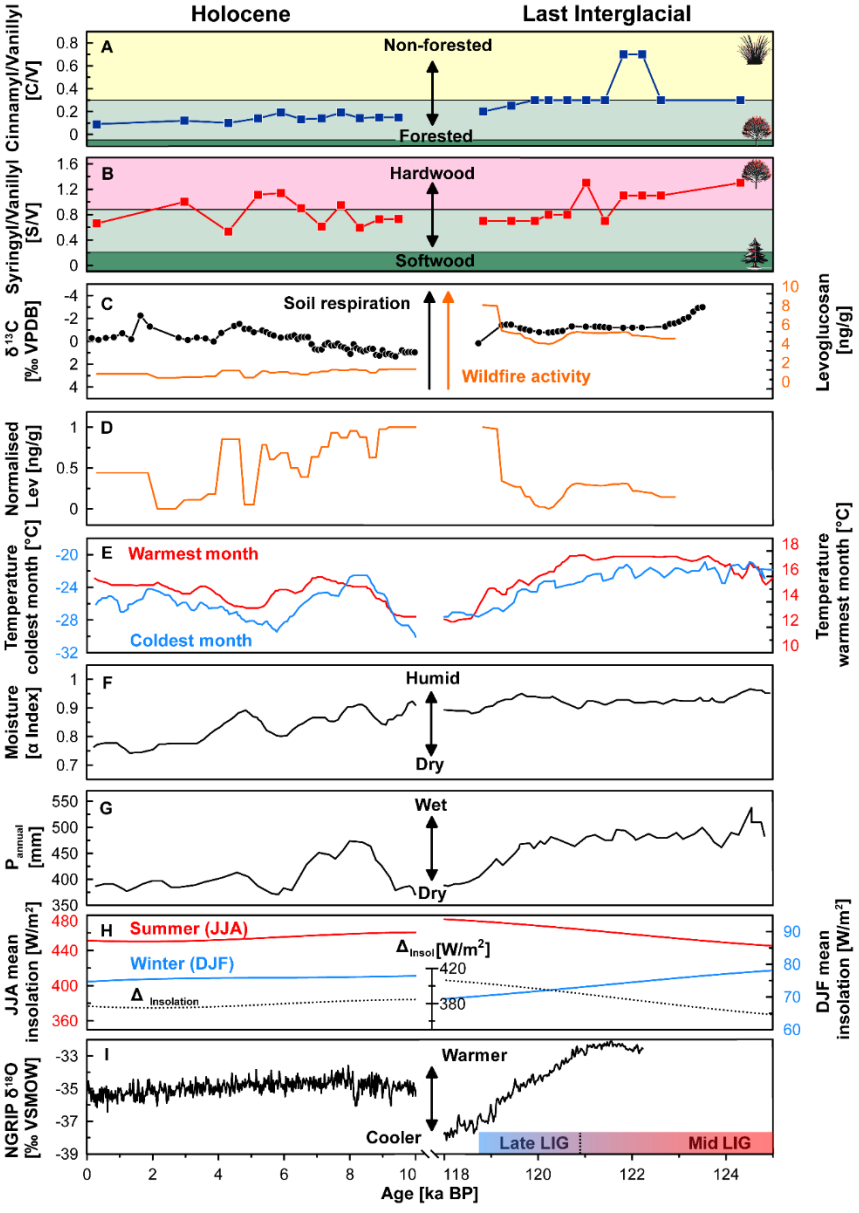

Figure 5: Vegetation (A, B), wildfire and climate (C, D) signals derived from Botovskaya cave shown with published regional and hemispheric records of vegetation and climate (E-I). (A) Dark green shading indicates predominantly forested vegetation, yellow shading open vegetation, and yellow/green mixed vegetation. (B) Pink shading indicates hardwood, dark green softwood and pink/green mixed vegetation. (C) The $\delta^{13}C$ record reflects local hydrological conditions and soil respiration, with lower values indicating wetter conditions and increased soil respiration. (D) Normalised levoglucosan levels highlight multi-centennial trends during the LIG and the Holocene. Lake Baikal pollen records (Tarasov et al., 2007) include temperatures of the warmest and coldest months (E), moisture (F), and annual precipitation (G). (H) Hemispheric mean insolation at 55.3°N of June – August (JJA) on left and December – February (DJF) on right, and Δ insolation (summer – winter) (Laskar et al. 2004) indicate changes in thermal seasonality. (I) The $\delta^{18}O$ ice core values from the North Greenland Ice Core Project (NGRIP) showing changes in Northern Hemisphere air temperature (Andersen et al., 2004).

https://doi.org/10.5194/egusphere-2024-1707
Preprint. Discussion started: 12 June 2024

4.2 Vegetation composition and wildfire activity during the Holocene

Reconstructed Holocene vegetation composition appears to resemble modern assemblage of trees and shrubs with mixed hard- and softwood taxa. Generally declining C/V values in the second half of the Holocene (Fig. 5 A) suggest, independent of hard- and softwood vegetation types, that the forests of the later Holocene became better established and denser. Fluctuating S/V values indicate a changing prevalence of hardwood and softwood species over much of the Holocene (Figs. 4 and 5 B).

Despite lower temperatures compared to the middle LIG (Fig. 5 E, I), hardwood species found some foothold, likely due to a longer growth season facilitated by higher insolation in both summer and winter (Fig. 5 H). Significantly lower Lev concentrations, compared to the LIG (Fig. 5 C) indicate reduced fire prevalence, with a general decrease over the Holocene. Reduced moisture availability during the Holocene (Fig. 5 F, G) relative to the LIG, suggests a drier summer season with fewer thunderstorms (the main source of warm-season rainfall); and consequently, a reduced chance of dry lightning.

While the Holocene fire activity appears subdued compared to the LIG, the normalised Lev record reveals pronounced multi-centennial scale variability, superimposed on the long-term trend (Fig. 5 D). Higher temperatures, moisture availability, and growth season precipitation (Fig. 5 E-G, I) during the Northern Hemisphere Holocene thermal maximum (Baker et al., 2017) likely facilitated more wildfires than during other portions of the Holocene. While higher moisture availability and increased wildfire activity seem, at first glance, counterintuitive, increased temperatures and moisture can increase biomass (fuel) availability that can increase vulnerability to wildfire activity (Marlon, 2020). The seasonal temperature contrast remained relatively stable over the course of the Holocene, compared to the late LIG (Fig. 5 H-I), which might have helped the establishment of denser forest cover. Our $\delta^{13}C$ record supports this interpretation as the transition from high $\delta^{13}C$ values in the early Holocene to more negative $\delta^{13}C$ values in the middle Holocene can be interpreted as improved soil development and higher respiration under forest cover.

To date, only one Holocene wildfire record is available from southern Siberia (Barhoumi et al., 2021). The reconstruction is based on charcoal occurrence in two lakes located to the immediate southeast of Lake Baikal, and suggests higher wildfire activity in the early Holocene, followed by an abrupt decline after 6.5 ka BP. Comparison with pollen records from the Lake Baikal region (Bezrukova et al., 2013; Demske et al., 2005; Shichi et al., 2009) indicates that this wildfire trend was likely related to a shift from predominantly Siberian spruce (*Picea obovata*) to pine trees (e.g., *Pinus sylvestris*), which drove a transition from mostly crown fires (entire trees) to more surface fires (surface litter and decaying understory) by the middle Holocene. While our record cannot identify wildfire intensity or estimate its vertical distribution (e.g., differentiating between

https://doi.org/10.5194/egusphere-2024-1707
Preprint. Discussion started: 12 June 2024

crown and surface fires), their reconstruction confirms a generally decreasing fire activity trend over the Holocene in the wider Baikal region (Fig. 5. C, D).

A slight increase in our Lev concentration record in the late Holocene (Fig. 5 D) may reflect either increasing natural wildfire prevalence or, possibly, an increasing anthropogenic component. Human populations have been well-established in the Baikal region since the last glacial (Weber et al., 2011; Shichi et al., 2023), with archaeological evidence (e.g., petroglyphs at Shishkino in the Lena valley) pointing to large river valleys, like that of the Angara and Lena, as main migration routes (Kılınç et al., 2021; Tolstoy, 1958; White et al., 2008). Although our Holocene record might be influenced by human activity, we caution that our dataset lacks the temporal resolution to identify anthropogenic impacts on fire occurrence. Increasing population density deep within Eurasia has been linked with elevated wildfire occurrence, and similar links might be found with early human settlements (White et al., 2008). However, the significantly higher wildfire activity in the late LIG period, with vegetation similar to the late Holocene, suggests that other factors, like warmer-than-modern surface temperatures and enhanced seasonal temperature contrasts play a more important role.

4.3 Comparison of wildfires and vegetation during the LIG and Holocene

Our data indicate that LIG and Holocene differed in terms of fire pattern. Fire *pattern* and fire *regime* are often used interchangeably and here we follow Bowman et al. (2020) and refer to fire *pattern* as the interplay between climate, vegetation type (fuel), and ignition (natural or related to human activity). Fire *regime* is defined as a typical range of fire frequency, type, intensity, severity, seasonality, and spatial scale (Cochrane and Bowman, 2021). Given the challenges in extracting these properties from speleothem (and other) archives, we limit our reconstruction to fire *pattern*.

Contrasting vegetation types (as wildfire fuel) between LIG and Holocene seem to play a crucial role in wildfire activity in southern Siberia. Open steppe vegetation is more flammable than closed forest, and hardwoods are generally more resistant to wildfire than softwoods. As vegetation type is inherently related to regional climate, disentangling the primary driver for changes in wildfire pattern is complex.

Our data suggest that during the LIG, fire activity increased with increasing seasonal temperature gradient. Fire ignition is more probable during warmer, drier summers in a steppe-like environment than in a forested landscape (Kharuk et al., 2021). High temperature and fuel availability are conducive for more frequent and severe wildfires. Seasonal hydrological dynamics are another important factor for wildfire activity, as the availability and temporal distribution of moisture during the growth season not only determines vegetation composition but also wildfire hazard (i.e., the likelihood of fire ignition by lightning).

Moisture supply to continental Eurasia via the westerlies depends on Atlantic Sea ice extent and atmospheric circulation pattern (Smith et al., 2016), which varied between the LIG and Holocene due to differences in meridional temperature gradients (Baker

https://doi.org/10.5194/egusphere-2024-1707
Preprint. Discussion started: 12 June 2024

et al., 2017). The Atlantic Multidecadal Oscillation has recently been found to influence wildfire regimes in northeast China via modulation of moisture supply and regional warming (Gao et al., 2021).

The relatively high $\delta^{13}C$ values (-2 to +1 ‰) during both the Holocene and LIG indicate a significant contribution from the host rock, rather than soil and vegetation overlying the cave. The very stable, and lower (compared to Holocene) $\delta^{13}C$ values in the middle to late LIG likely reflect higher regional temperatures, as suggested by Fohlmeister et al. (2020) for environments with low (<800 mm/a) annual precipitation. High wildfire activity and non-woody taxa during the LIG (Fig. 5A-C) align well with these dry and warm conditions. Soil respiration diminished further in the late LIG when sea ice (and eventually Scandinavian ice) build-up limited eastward moisture transport, as evidenced by the high $\delta^{13}C$ value at the end of our LIG record (ca. 119 ka BP).

Higher stalagmite $\delta^{13}C$ values during the early Holocene might result from more episodic summer rainfall, and generally drier warm season conditions with reduced soil respiration. These drier episodes induced a vegetation shift to more softwood, mostly mixed woody and non-woody vegetation, and higher wildfire activity as a consequence of increased fuel availability that promoted dry-lightning efficiency.

Considering the differences in vegetation dynamics, insolation, and moisture availability, the LIG is not an adequate analogue for the Holocene. However, with increasingly drier and warmer continental summers as a result of global warming (Zhang et al., 2020), and independent of orbital parameters, the boreal forest zone is likely to be more frequently exposed to summer heat waves that promote fire weather (Hessilt et al., 2022). Such conditions, enhanced by ongoing forest loss and vegetation shifts linked to wildfires, will likely fuel a positive feedback loop and further increase fire activity in the Eurasian boreal forest.

5. Conclusions

Stalagmite-derived levoglucosan (Lev) concentrations and lignin oxidation products (S/V and C/V ratios) allowed reconstruction of last interglacial (LIG) and Holocene wildfire and vegetation dynamics in southern Siberia. In the region, dry-lightning is the most probable natural ignition mechanisms of wildfires. Consequently, we have focused on two other elements of the fire triangle: vegetation (fuel) and climate. Our results document diverse landscapes surrounding Botovskaya cave in the LIG and Holocene. The LIG was characterised by a mix of steppe and forest vegetation fuelling frequent and sustained wildfires. A gradual increase in seasonal temperature gradient and regional drying accompanied by transition from fire-resilient hardwood to fire-vulnerable softwood taxa were likely reasons for increased fire activity towards the end of the LIG. In contrast to the LIG, forest vegetation established during the Holocene, with ongoing competition between hard- and softwood taxa. The mixed nature of Holocene forests, likely related to generally cooler Holocene temperatures and subdued seasonal temperature contrast, appears to have reduced wildfire activity than the LIG. While the wildfire activity varied over the course

https://doi.org/10.5194/egusphere-2024-1707
Preprint. Discussion started: 12 June 2024

of the Holocene, the amplitude and absolute values were much smaller compared to the LIG. We propose that the composition of the vegetation and the thermal contrast between the seasons are the most important natural drivers of Siberian wildfires. Under continued global warming, increasing summer temperatures and dryness are likely to promote more frequent wildfires with escalating societal and ecological repercussions.

Data availability. All results from this study are available in the Supplement to this publication.

Author contributions. Study design: JM, SB, JH; methodology and data acquisition: JM, SB, JH, GN, FL, AV; original draft preparation; JM; writing and editing; JM, SB, OK, AG, SU, FL, GN, TH, AV, AK, AO, AM, GH.

Competing interests. The authors declare that they have no conflict of interest.

Acknowledgements. Thanks to members of Speleoclub Arabika and Tobias Braun for their help during fieldwork in Siberia, and to Hamish Couper for help with laboratory work for U/Th dating. Thanks also go to Pavel Tarasov, Sina Longman, Frederic Wilson, and Natalie Latysh, for providing helpful comments on the manuscript. Any use of trade, firm, or product names is for descriptive purposes only and does not imply endorsement by the U.S. Government.

Financial support. This work was funded by the Leverhulme Trust (IsoPerm project – RPG-20202-334), NERC Fellowship (NE/G013829/1, NERC Standard G), OnePlanet DTP (NE/S007512/1), and the German Research Foundation (HO 1748/20-1).

References

Andersen, K. K., Azuma, N., Barnola, J.-M., Bigler, M., Biscaye, P., Caillon, N., Chappellaz, J., Clausen, H. B., Dahl-Jensen, D., Fischer, H., Flückiger, J., Fritzsche, D., Fujii, Y., Goto-Azuma, K., Grønvold, K., Gundestrup, N. S., Hansson, M., Huber, C., Hvidberg, C. S., Johnsen, S. J., Jonsell, U., Jouzel, J., Kipfstuhl, S., Landais, A., Leuenberger, M., Lorrain, R., Masson-Delmotte, V., Miller, H., Motoyama, H., Narita, H., Popp, T., Rasmussen, S. O., Raynaud, D., Rothlisberger, R., Ruth, U., Samyn, D., Schwander, J., Shoji, H., Siggard-Andersen, M.-L., Steffensen, J. P., Stocker, T., Sveinbjörnsdóttir, A. E., Svensson, A., Takata, M., Tison, J.-L., Thorsteinsson, Th., Watanabe, O., Wilhelms, F., White, J. W. C., and North Greenland Ice Core Project members: High-resolution record of Northern Hemisphere climate extending into the last interglacial period, Nature, 431, 147–151, https://doi.org/10.1038/nature02805, 2004.

Armstrong McKay, D. I., Staal, A., Abrams, J. F., Winkelmann, R., Sakschewski, B., Loriani, S., Fetzer, I., Cornell, S. E., Rockström, J., and Lenton, T. M.: Exceeding 1.5°C global warming could trigger multiple climate tipping points, Science, 377, eabn7950, https://doi.org/10.1126/science.abn7950, 2022.

https://doi.org/10.5194/egusphere-2024-1707
Preprint. Discussion started: 12 June 2024

Baker, J. L., Lachniet, M. S., Chervyatsova, O., Asmerom, Y., and Polyak, V. J.: Holocene warming in western continental Eurasia driven by glacial retreat and greenhouse forcing, Nature Geosci, 10, 430–435, https://doi.org/10.1038/ngeo2953, 2017.

Balzter, H., Gerard, F., George, C., Weedon, G., Grey, W., Combal, B., Bartholomé, E., Bartalev, S., and Los, S.: Coupling of Vegetation Growing Season Anomalies and Fire Activity with Hemispheric and Regional-Scale Climate Patterns in Central and East Siberia, Journal of Climate, 20, 3713–3729, https://doi.org/10.1175/JCLI4226, 2007.

Barhoumi, C., Vogel, M., Dugerdil, L., Limani, H., Joannin, S., Peyron, O., and Ali, A. A.: Holocene Fire Regime Changes in the Southern Lake Baikal Region Influenced by Climate-Vegetation-Anthropogenic Activity Interactions, Forests, 12, 978, https://doi.org/10.3390/f12080978, 2021.

Belcher, C. M., Mills, B. J. W., Vitali, R., Baker, S. J., Lenton, T. M., and Watson, A. J.: The rise of angiosperms strengthened fire feedbacks and improved the regulation of atmospheric oxygen, Nat Commun, 12, 503, https://doi.org/10.1038/s41467-020-20772-2, 2021.

Bezrukova, E. V., Hildebrandt, S., Letunova, P. P., Ivanov, E. V., Orlova, L. A., Müller, S., and Tarasov, P. E.: Vegetation dynamics around Lake Baikal since the middle Holocene reconstructed from the pollen and botanical composition analyses of peat sediments: Implications for paleoclimatic and archeological research, Quaternary International, 290–291, 35–45, https://doi.org/10.1016/j.quaint.2012.10.043, 2013.

Bondur, V. G., Gordo, K. A., Voronova, O. S., Zima, A. L., and Feoktistova, N. V.: Intense Wildfires in Russia over a 22-Year Period According to Satellite Data, Fire, 6, 99, https://doi.org/10.3390/fire6030099, 2023.

Bowman, D. M. J. S., Kolden, C. A., Abatzoglou, J. T., Johnston, F. H., van der Werf, G. R., and Flannigan, M.: Vegetation fires in the Anthropocene, Nat Rev Earth Environ, 1, 500–515, https://doi.org/10.1038/s43017-020-0085-3, 2020.

Brazhnik, K., Hanley, C., and Shugart, H. H.: Simulating Changes in Fires and Ecology of the 21st Century Eurasian Boreal Forests of Siberia, Forests, 8, 49, https://doi.org/10.3390/f8020049, 2017.

Breitenbach, S. F. M. and Bernasconi, S. M.: Carbon and oxygen isotope analysis of small carbonate samples (20 to 100 µg) with a GasBench II preparation device, Rapid Communications in Mass Spectrometry, 25, 1910–1914, https://doi.org/10.1002/rcm.5052, 2011.

Breitenbach, S. F. M., Rehfeld, K., Goswami, B., Baldini, J. U. L., Ridley, H. E., Kennett, D. J., Prufer, K. M., Aquino, V. V., Asmerom, Y., Polyak, V. J., Cheng, H., Kurths, J., and Marwan, N.: COnstructing Proxy Records from Age models (COPRA), Climate of the Past, 8, 1765–1779, https://doi.org/10.5194/cp-8-1765-2012, 2012.

Brunello, C. F., Andermann, C., Helle, G., Comiti, F., Tonon, G., Tiwari, A., and Hovius, N.: Hydroclimatic seasonality recorded by tree ring δ18O signature across a Himalayan altitudinal transect, Earth and Planetary Science Letters, 518, 148–159, https://doi.org/10.1016/j.epsl.2019.04.030, 2019.

Bryukhanov, A. V., Panov, A. V., Ponomarev, E. I., and Sidenko, N. V.: Wildfire Impact on the Main Tree Species of the Near-Yenisei Siberia, Izv. Atmos. Ocean. Phys., 54, 1525–1533, https://doi.org/10.1134/S0001433818110026, 2018.

Capron, E., Govin, A., Stone, E. J., Masson-Delmotte, V., Mulitza, S., Otto-Bliesner, B., Rasmussen, T. L., Sime, L. C., Waelbroeck, C., and Wolff, E. W.: Temporal and spatial structure of multi-millennial temperature changes at high latitudes

https://doi.org/10.5194/egusphere-2024-1707
Preprint. Discussion started: 12 June 2024

during the Last Interglacial, Quaternary Science Reviews, 103, 116–133, https://doi.org/10.1016/j.quascirev.2014.08.018, 2014.

Ciavarella, A., Cotterill, D., Stott, P., Kew, S., Philip, S., van Oldenborgh, G. J., Skålevåg, A., Lorenz, P., Robin, Y., Otto, F., Hauser, M., Seneviratne, S. I., Lehner, F., and Zolina, O.: Prolonged Siberian heat of 2020 almost impossible without human influence, Climatic Change, 166, 9, https://doi.org/10.1007/s10584-021-03052-w, 2021.

Cochrane, M. A. and Bowman, D. M. J. S.: Manage fire regimes, not fires, Nat. Geosci., 14, 455–457, https://doi.org/10.1038/s41561-021-00791-4, 2021.

Demske, D., Heumann, G., Granoszewski, W., Nita, M., Mamakowa, K., Tarasov, P. E., and Oberhänsli, H.: Late glacial and Holocene vegetation and regional climate variability evidenced in high-resolution pollen records from Lake Baikal, Global and Planetary Change, 46, 255–279, https://doi.org/10.1016/j.gloplacha.2004.09.020, 2005.

Dietze, E., Mangelsdorf, K., Andreev, A., Karger, C., Schreuder, L. T., Hopmans, E. C., Rach, O., Sachse, D., Wennrich, V., and Herzschuh, U.: Relationships between low-temperature fires, climate and vegetation during three late glacials and interglacials of the last 430 kyr in northeastern Siberia reconstructed from monosaccharide anhydrides in Lake El'gygytgyn sediments, Climate of the Past, 16, 799–818, https://doi.org/10.5194/cp-16-799-2020, 2020.

Dolman, A. J., Shvidenko, A., Schepaschenko, D., Ciais, P., Tchebakova, N., Chen, T., van der Molen, M. K., Belelli Marchesini, L., Maximov, T. C., Maksyutov, S., and Schulze, E.-D.: An estimate of the terrestrial carbon budget of Russia using inventory-based, eddy covariance and inversion methods, Biogeosciences, 9, 5323–5340, https://doi.org/10.5194/bg-9-5323-2012, 2012.

Eichler, A., Tinner, W., Brütsch, S., Olivier, S., Papina, T., and Schwikowski, M.: An ice-core based history of Siberian forest fires since AD 1250, Quaternary Science Reviews, 30, 1027–1034, https://doi.org/10.1016/j.quascirev.2011.02.007, 2011.

Elias, V. O., Simoneit, B. R. T., Cordeiro, R. C., and Turcq, B.: Evaluating levoglucosan as an indicator of biomass burning in Carajás, amazônia: a comparison to the charcoal record22Associate editor: R. Summons, Geochimica et Cosmochimica Acta, 65, 267–272, https://doi.org/10.1016/S0016-7037(00)00522-6, 2001.

Fohlmeister, J., Arps, J., Spötl, C., Schröder-Ritzrau, A., Plessen, B., Günter, C., Frank, N., and Trüssel, M.: Carbon and oxygen isotope fractionation in the water-calcite-aragonite system, Geochimica et Cosmochimica Acta, 235, 127–139, https://doi.org/10.1016/j.gca.2018.05.022, 2018.

Forkel, M., Thonicke, K., Beer, C., Cramer, W., Bartalev, S., and Schmullius, C.: Extreme fire events are related to previous-year surface moisture conditions in permafrost-underlain larch forests of Siberia, Environ. Res. Lett., 7, 044021, https://doi.org/10.1088/1748-9326/7/4/044021, 2012.

García-Lázaro, J. R., Moreno-Ruiz, J. A., Riaño, D., and Arbelo, M.: Estimation of Burned Area in the Northeastern Siberian Boreal Forest from a Long-Term Data Record (LTDR) 1982–2015 Time Series, Remote Sensing, 10, 940, https://doi.org/10.3390/rs10060940, 2018.

https://doi.org/10.5194/egusphere-2024-1707
Preprint. Discussion started: 12 June 2024

Glückler, R., Herzschuh, U., Kruse, S., Andreev, A., Vyse, S. A., Winkler, B., Biskaborn, B. K., Pestryakova, L., and Dietze, E.: Wildfire history of the boreal forest of south-western Yakutia (Siberia) over the last two millennia documented by a lake-sediment charcoal record, Biogeosciences, 18, 4185–4209, https://doi.org/10.5194/bg-18-4185-2021, 2021.

Glückler, R., Geng, R., Grimm, L., Baisheva, I., Herzschuh, U., Stoof-Leichsenring, K. R., Kruse, S., Andreev, A., Pestryakova, L., and Dietze, E.: Holocene wildfire and vegetation dynamics in Central Yakutia, Siberia, reconstructed from lake-sediment proxies, Frontiers in Ecology and Evolution, 10, 2022.

Hantemirov, R. M., Corona, C., Guillet, S., Shiyatov, S. G., Stoffel, M., Osborn, T. J., Melvin, T. M., Gorlanova, L. A., Kukarskih, V. V., Surkov, A. Y., von Arx, G., and Fonti, P.: Current Siberian heating is unprecedented during the past seven millennia, Nat Commun, 13, 4968, https://doi.org/10.1038/s41467-022-32629-x, 2022.

Hedges, J. I. and Mann, D. C.: The characterization of plant tissues by their lignin oxidation products, Geochimica et Cosmochimica Acta, 43, 1803–1807, https://doi.org/10.1016/0016-7037(79)90028-0, 1979.

Heidke, I., Scholz, D., and Hoffmann, T.: Quantification of lignin oxidation products as vegetation biomarkers in speleothems and cave drip water, Biogeosciences, 15, 5831–5845, https://doi.org/10.5194/bg-15-5831-2018, 2018.

Hessilt, T. D., Abatzoglou, J. T., Chen, Y., Randerson, J. T., Scholten, R. C., Werf, G. van der, and Veraverbeke, S.: Future increases in lightning ignition efficiency and wildfire occurrence expected from drier fuels in boreal forest ecosystems of western North America, Environ. Res. Lett., 17, 054008, https://doi.org/10.1088/1748-9326/ac6311, 2022.

Homann, J., Oster, J. L., de Wet, C. B., Breitenbach, S. F. M., and Hoffmann, T.: Linked fire activity and climate whiplash in California during the early Holocene, Nat Commun, 13, 7175, https://doi.org/10.1038/s41467-022-34950-x, 2022.

Homann, J., Karbach, N., Carolin, S. A., James, D. H., Hodell, D., Breitenbach, S. F. M., Kwiecien, O., Brenner, M., Peraza Lope, C., and Hoffmann, T.: Past fire dynamics inferred from polycyclic aromatic hydrocarbons and monosaccharide anhydrides in a stalagmite from the archaeological site of Mayapan, Mexico, Biogeosciences, 20, 3249–3260, https://doi.org/10.5194/bg-20-3249-2023, 2023.

Jex, C. N., Pate, G. H., Blyth, A. J., Spencer, R. G. M., Hernes, P. J., Khan, S. J., and Baker, A.: Lignin biogeochemistry: from modern processes to Quaternary archives, Quaternary Science Reviews, 87, 46–59, https://doi.org/10.1016/j.quascirev.2013.12.028, 2014.

Kamp, U., Walther, M., and Dashtseren, A.: Mongolia's cryosphere, Geomorphology, 410, 108202, https://doi.org/10.1016/j.geomorph.2022.108202, 2022.

Kharuk, V. I., Ponomarev, E. I., Ivanova, G. A., Dvinskaya, M. L., Coogan, S. C. P., and Flannigan, M. D.: Wildfires in the Siberian taiga, Ambio, 50, 1953–1974, https://doi.org/10.1007/s13280-020-01490-x, 2021a.

Kharuk, V. I., Ponomarev, E. I., Ivanova, G. A., Dvinskaya, M. L., Coogan, S. C. P., and Flannigan, M. D.: Wildfires in the Siberian taiga, Ambio, 50, 1953–1974, https://doi.org/10.1007/s13280-020-01490-x, 2021b.

Kharuk, V. I., Shvetsov, E. G., Buryak, L. V., Golyukov, A. S., Dvinskaya, M. L., and Petrov, I. A.: Wildfires in the Larch Range within Permafrost, Siberia, Fire, 6, 301, https://doi.org/10.3390/fire6080301, 2023.

Kılınç, G. M., Kashuba, N., Koptekin, D., Bergfeldt, N., Dönertaş, H. M., Rodríguez-Varela, R., Shergin, D., Ivanov, G., Kichigin, D., Pestereva, K., Volkov, D., Mandryka, P., Kharinskii, A., Tishkin, A., Ineshin, E., Kovychev, E., Stepanov, A., Dalén, L., Günther, T., Kırdök, E., Jakobsson, M., Somel, M., Krzewińska, M., Storå, J., and Götherström, A.: Human population dynamics and Yersinia pestis in ancient northeast Asia, Science Advances, 7, eabc4587, https://doi.org/10.1126/sciadv.abc4587, 2021.

Klein Tank, A. M. G., Wijngaard, J. B., Können, G. P., Böhm, R., Demarée, G., Gocheva, A., Mileta, M., Pashiardis, S., Hejkrlik, L., Kern-Hansen, C., Heino, R., Bessemoulin, P., Müller-Westermeier, G., Tzanakou, M., Szalai, S., Pálsdóttir, T., Fitzgerald, D., Rubin, S., Capaldo, M., Maugeri, M., Leitass, A., Bukantis, A., Aberfeld, R., van Engelen, A. F. V., Forland, E., Mietus, M., Coelho, F., Mares, C., Razuvaev, V., Nieplova, E., Cegnar, T., Antonio López, J., Dahlström, B., Moberg, A., Kirchhofer, W., Ceylan, A., Pachaliuk, O., Alexander, L. V., and Petrovic, P.: Daily dataset of 20th-century surface air temperature and precipitation series for the European Climate Assessment, International Journal of Climatology, 22, 1441–1453, https://doi.org/10.1002/joc.773, 2002.

Kostrova, S. S., Meyer, H., Fernandoy, F., Werner, M., and Tarasov, P. E.: Moisture origin and stable isotope characteristics of precipitation in southeast Siberia, Hydrological Processes, 34, 51–67, https://doi.org/10.1002/hyp.13571, 2020.

Laaha, G., Gauster, T., Tallaksen, L. M., Vidal, J.-P., Stahl, K., Prudhomme, C., Heudorfer, B., Vlnas, R., Ionita, M., Van Lanen, H. A. J., Adler, M.-J., Caillouet, L., Delus, C., Fendekova, M., Gailliez, S., Hannaford, J., Kingston, D., Van Loon, A. F., Mediero, L., Osuch, M., Romanowicz, R., Sauquet, E., Stagge, J. H., and Wong, W. K.: The European 2015 drought from a hydrological perspective, Catchment hydrology/Stochastic approaches, https://doi.org/10.5194/hess-2016-366, 2016.

Lechleitner, F. A., Mason, A. J., Breitenbach, S. F. M., Vaks, A., Haghipour, N., and Henderson, G. M.: Permafrost-related hiatuses in stalagmites: Evaluating the potential for reconstruction of carbon cycle dynamics, Quaternary Geochronology, 56, 101037, https://doi.org/10.1016/j.quageo.2019.101037, 2020.

Lugina, K., Groisman, P., Vinnikov, K., Koknaeva, V., and Speranskaya, N.: Monthly Surface Air Temperature Time Series Area-Averaged Over the 30-Degree Latitudinal Belts of the Globe, https://doi.org/10.3334/CDIAC/CLI.003, 2006.

Marlon, J. R.: What the past can say about the present and future of fire, Quaternary Research, 96, 66–87, https://doi.org/10.1017/qua.2020.48, 2020.

Masyagina, O. V. and Menyailo, O. V.: The impact of permafrost on carbon dioxide and methane fluxes in Siberia: A meta-analysis, Environmental Research, 182, 109096, https://doi.org/10.1016/j.envres.2019.109096, 2020.

Obu, J., Westermann, S., Bartsch, A., Berdnikov, N., Christiansen, H. H., Dashtseren, A., Delaloye, R., Elberling, B., Etzelmüller, B., Kholodov, A., Khomutov, A., Kääb, A., Leibman, M. O., Lewkowicz, A. G., Panda, S. K., Romanovsky, V., Way, R. G., Westergaard-Nielsen, A., Wu, T., Yamkhin, J., and Zou, D.: Northern Hemisphere permafrost map based on TTOP modelling for 2000–2016 at 1 km2 scale, Earth-Science Reviews, 193, 299–316, https://doi.org/10.1016/j.earscirev.2019.04.023, 2019.

Peel, M. C., Finlayson, B. L., and McMahon, T. A.: Updated world map of the Köppen-Geiger climate classification, Hydrology and Earth System Sciences, 11, 1633–1644, https://doi.org/10.5194/hess-11-1633-2007, 2007.

https://doi.org/10.5194/egusphere-2024-1707
Preprint. Discussion started: 12 June 2024

Ponomarev, E., Yakimov, N., Ponomareva, T., Yakubailik, O., and Conard, S. G.: Current Trend of Carbon Emissions from Wildfires in Siberia, Atmosphere, 12, 559, https://doi.org/10.3390/atmos12050559, 2021.

Ponomarev, E., I., Kharuk, V. I., and Ranson, K. J.: Wildfires Dynamics in Siberian Larch Forests, Forests, 7, 125, https://doi.org/10.3390/f7060125, 2016.

Prokopenko, A. A., Williams, D. F., Karabanov, E. B., and Khursevich, G. K.: Continental response to Heinrich events and Bond cycles in sedimentary record of Lake Baikal, Siberia, Global and Planetary Change, 28, 217–226, https://doi.org/10.1016/S0921-8181(00)00074-6, 2001.

Rosbakh, S., Hartig, F., Sandanov, D. V., Bukharova, E. V., Miller, T. K., and Primack, R. B.: Siberian plants shift their phenology in response to climate change, Global Change Biology, 27, 4435–4448, https://doi.org/10.1111/gcb.15744, 2021.

Schuur, E. A. G., Abbott, B. W., Commane, R., Ernakovich, J., Euskirchen, E., Hugelius, G., Grosse, G., Jones, M., Koven, C., Leshyk, V., Lawrence, D., Loranty, M. M., Mauritz, M., Olefeldt, D., Natali, S., Rodenhizer, H., Salmon, V., Schädel, C., Strauss, J., Treat, C., and Turetsky, M.: Permafrost and Climate Change: Carbon Cycle Feedbacks From the Warming Arctic, Annual Review of Environment and Resources, 47, 343–371, https://doi.org/10.1146/annurev-environ-012220-011847, 2022.

Segato, D., Villoslada Hidalgo, M. D. C., Edwards, R., Barbaro, E., Vallelonga, P., Kjær, H. A., Simonsen, M., Vinther, B., Maffezzoli, N., Zangrando, R., Turetta, C., Battistel, D., Vésteinsson, O., Barbante, C., and Spolaor, A.: Five thousand years of fire history in the high North Atlantic region: natural variability and ancient human forcing, Climate of the Past, 17, 1533–1545, https://doi.org/10.5194/cp-17-1533-2021, 2021.

Senande-Rivera, M., Insua-Costa, D., and Miguez-Macho, G.: Spatial and temporal expansion of global wildland fire activity in response to climate change, Nat Commun, 13, 1208, https://doi.org/10.1038/s41467-022-28835-2, 2022.

Shichi, K., Takahara, H., Krivonogov, S. K., Bezrukova, E. V., Kashiwaya, K., Takehara, A., and Nakamura, T.: Late Pleistocene and Holocene vegetation and climate records from Lake Kotokel, central Baikal region, Quaternary International, 205, 98–110, https://doi.org/10.1016/j.quaint.2009.02.005, 2009.

Shichi, K., Goebel, T., Izuho, M., and Kashiwaya, K.: Climate amelioration, abrupt vegetation recovery, and the dispersal of Homo sapiens in Baikal Siberia, Science Advances, 9, eadi0189, https://doi.org/10.1126/sciadv.adi0189, 2023.

Shvetsov, E. G., Kukavskaya, E. A., Buryak, L. V., and Barrett, K.: Assessment of post-fire vegetation recovery in Southern Siberia using remote sensing observations, Environ. Res. Lett., 14, 055001, https://doi.org/10.1088/1748-9326/ab083d, 2019.

Simoneit, B. R. T.: Biomass burning — a review of organic tracers for smoke from incomplete combustion, Applied Geochemistry, 17, 129–162, https://doi.org/10.1016/S0883-2927(01)00061-0, 2002.

Simoneit, B. R. T., Schauer, J. J., Nolte, C. G., Oros, D. R., Elias, V. O., Fraser, M. P., Rogge, W. F., and Cass, G. R.: Levoglucosan, a tracer for cellulose in biomass burning and atmospheric particles, Atmospheric Environment, 33, 173–182, https://doi.org/10.1016/S1352-2310(98)00145-9, 1999.

Spötl, C.: A simple method of soil gas stable carbon isotope analysis, Rapid Communications in Mass Spectrometry, 18, 1239–1242, https://doi.org/10.1002/rcm.1468, 2004.

https://doi.org/10.5194/egusphere-2024-1707
Preprint. Discussion started: 12 June 2024

Steffen, W., Rockström, J., Richardson, K., Lenton, T. M., Folke, C., Liverman, D., Summerhayes, C. P., Barnosky, A. D., Cornell, S. E., Crucifix, M., Donges, J. F., Fetzer, I., Lade, S. J., Scheffer, M., Winkelmann, R., and Schellnhuber, H. J.: Trajectories of the Earth System in the Anthropocene, Proceedings of the National Academy of Sciences, 115, 8252–8259, https://doi.org/10.1073/pnas.1810141115, 2018.

Sun, Q., Burrell, A., Barrett, K., Kukavskaya, E., Buryak, L., Kaduk, J., and Baxter, R.: Climate Variability May Delay Post-Fire Recovery of Boreal Forest in Southern Siberia, Russia, Remote Sensing, 13, 2247, https://doi.org/10.3390/rs13122247, 2021.

Swain, D. L.: A Shorter, Sharper Rainy Season Amplifies California Wildfire Risk, Geophysical Research Letters, 48, e2021GL092843, https://doi.org/10.1029/2021GL092843, 2021.

Talucci, A. C., Loranty, M. M., and Alexander, H. D.: Siberian taiga and tundra fire regimes from 2001–2020, Environ. Res. Lett., 17, 025001, https://doi.org/10.1088/1748-9326/ac3f07, 2022.

Tchebakova, N. M., Parfenova, E., and Soja, A. J.: The effects of climate, permafrost and fire on vegetation change in Siberia in a changing climate, Environ. Res. Lett., 4, 045013, https://doi.org/10.1088/1748-9326/4/4/045013, 2009.

Tchebakova, N. M., Rehfeldt, G. E., and Parfenova, E. I.: From Vegetation Zones to Climatypes: Effects of Climate Warming on Siberian Ecosystems, in: Permafrost Ecosystems, vol. 209, edited by: Osawa, A., Zyryanova, O. A., Matsuura, Y., Kajimoto, T., and Wein, R. W., Springer Netherlands, Dordrecht, 427–446, https://doi.org/10.1007/978-1-4020-9693-8_22, 2010.

Tepley, A. J., Thomann, E., Veblen, T. T., Perry, G. L. W., Holz, A., Paritsis, J., Kitzberger, T., and Anderson-Teixeira, K. J.: Influences of fire–vegetation feedbacks and post-fire recovery rates on forest landscape vulnerability to altered fire regimes, Journal of Ecology, 106, 1925–1940, https://doi.org/10.1111/1365-2745.12950, 2018.

Tolstoy, P.: The Archaeology of the Lena Basin and Its New World Relationships, Part II, American Antiquity, 24, 63–81, https://doi.org/10.2307/276742, 1958.

Tomshin, O. and Solovyev, V.: Spatio-temporal patterns of wildfires in Siberia during 2001–2020, Geocarto International, 37, 7339–7357, https://doi.org/10.1080/10106049.2021.1973581, 2022.

Turney, C. S. M. and Jones, R. T.: Does the Agulhas Current amplify global temperatures during super-interglacials?, Journal of Quaternary Science, 25, 839–843, https://doi.org/10.1002/jqs.1423, 2010.

Vaks, A., Gutareva, O. S., Breitenbach, S. F. M., Avirmed, E., Mason, A. J., Thomas, A. L., Osinzev, A. V., Kononov, A. M., and Henderson, G. M.: Speleothems reveal 500,000-year history of Siberian permafrost, Science, 340, 183–186, https://doi.org/10.1126/science.1228729, 2013.

Vaks, A., Mason, A. J., Breitenbach, S. F. M., Kononov, A. M., Osinzev, A. V., Rosensaft, M., Borshevsky, A., Gutareva, O. S., and Henderson, G. M.: Palaeoclimate evidence of vulnerable permafrost during times of low sea ice, Nature, 577, 221–225, https://doi.org/10.1038/s41586-019-1880-1, 2020.

Walker, X. J., Baltzer, J. L., Cumming, S. G., Day, N. J., Ebert, C., Goetz, S., Johnstone, J. F., Potter, S., Rogers, B. M., Schuur, E. A. G., Turetsky, M. R., and Mack, M. C.: Increasing wildfires threaten historic carbon sink of boreal forest soils, Nature, 572, 520–523, https://doi.org/10.1038/s41586-019-1474-y, 2019.

https://doi.org/10.5194/egusphere-2024-1707
Preprint. Discussion started: 12 June 2024

Weber, A. W., White, D., Bazaliiskii, V. I., Goriunova, O. I., Savel'ev, N. A., and Anne Katzenberg, M.: Hunter–gatherer foraging ranges, migrations, and travel in the middle Holocene Baikal region of Siberia: Insights from carbon and nitrogen stable isotope signatures, Journal of Anthropological Archaeology, 30, 523–548, https://doi.org/10.1016/j.jaa.2011.06.006, 2011.

Westerling, A. L., Hidalgo, H. G., Cayan, D. R., and Swetnam, T. W.: Warming and Earlier Spring Increase Western U.S. Forest Wildfire Activity, Science, 313, 940–943, https://doi.org/10.1126/science.1128834, 2006.

White, D., Preece, R. C., Shchetnikov, A. A., Parfitt, S. A., and Dlussky, K. G.: A Holocene molluscan succession from floodplain sediments of the upper Lena River (Lake Baikal region), Siberia, Quaternary Science Reviews, 27, 962–987, https://doi.org/10.1016/j.quascirev.2008.01.010, 2008.

Zennaro, P., Kehrwald, N., McConnell, J. R., Schüpbach, S., Maselli, O. J., Marlon, J., Vallelonga, P., Leuenberger, D., Zangrando, R., Spolaor, A., Borrotti, M., Barbaro, E., Gambaro, A., and Barbante, C.: Fire in ice: two millennia of boreal forest fire history from the Greenland NEEM ice core, Climate of the Past, 10, 1905–1924, https://doi.org/10.5194/cp-10-1905-2014, 2014.

Zhang, P., Jeong, J.-H., Yoon, J.-H., Kim, H., Wang, S.-Y. S., Linderholm, H. W., Fang, K., Wu, X., and Chen, D.: Abrupt shift to hotter and drier climate over inner East Asia beyond the tipping point, Science, 370, 1095–1099, https://doi.org/10.1126/science.abb3368, 2020.

https://doi.org/10.5194/egusphere-2024-1707
Preprint. Discussion started: 12 June 2024

Appendices

Appendix A

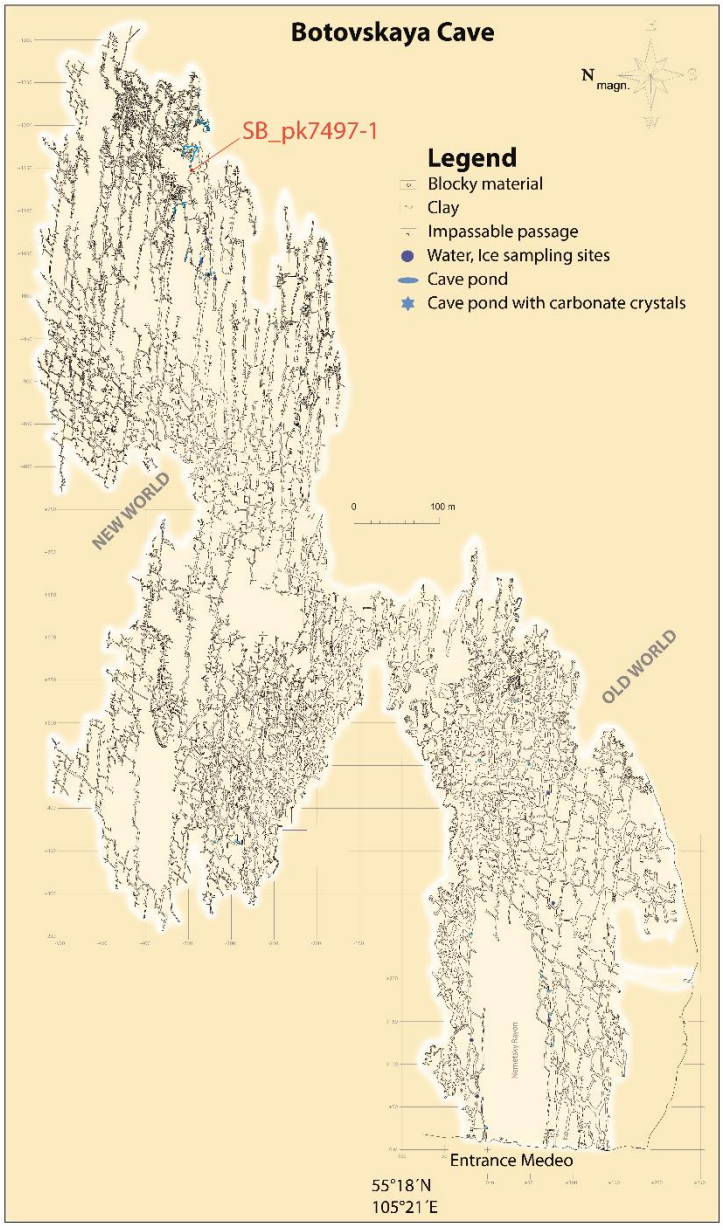

Fig. A1: Mapped areas of Botovskaya cave with locations of specimen. Old and New world regions are joined by a route 650 m into the cave. The location of sample SB_PK7497-1 is highlighted in the northeastern part of the New World. Key features are listed within the figure.

https://doi.org/10.5194/egusphere-2024-1707
Preprint. Discussion started: 12 June 2024

Appendix B

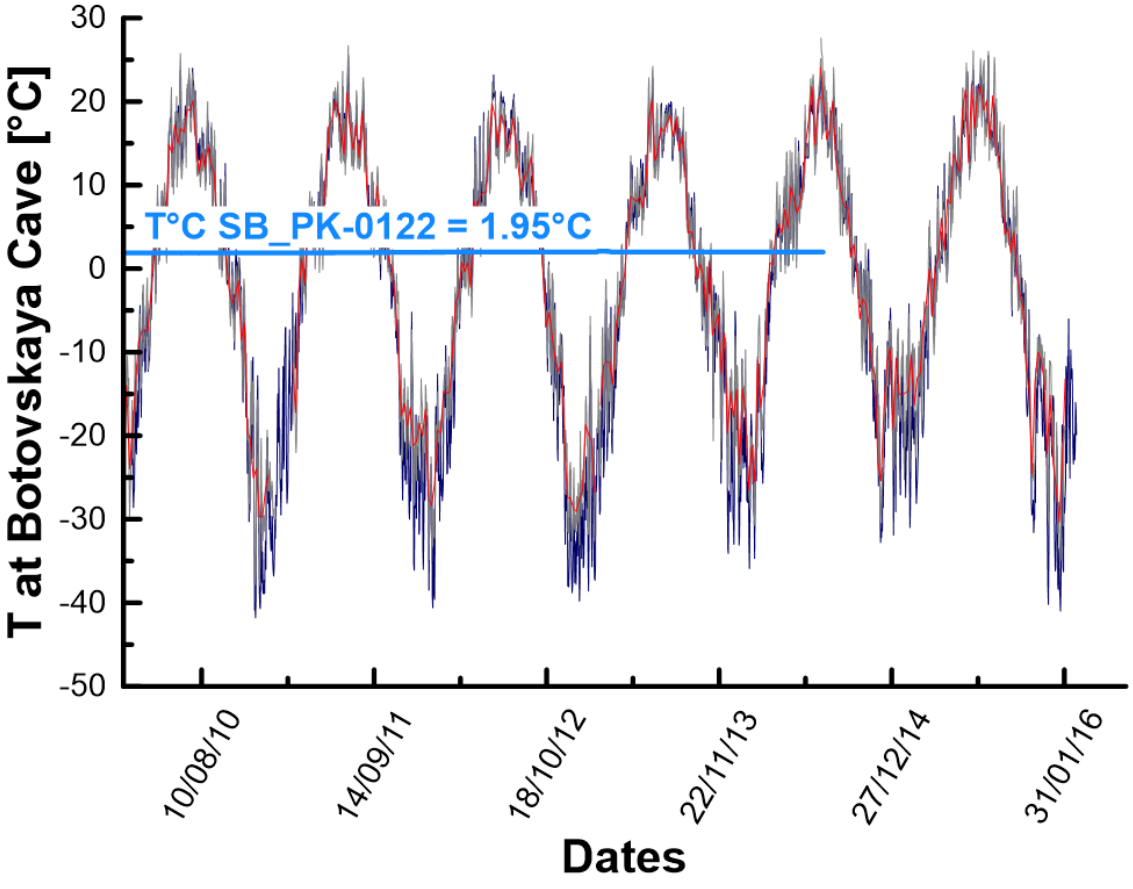

Fig. B1: Temperatures recorded inside (blue line) and outside (grey and red lines) Botovskaya cave over a period of 6 years. Trends of both daily (grey line) and weekly average (red line) temperatures outside the cave are increasing since 2013, whereas inside cave temperatures remain stable. Average daily temperatures for Zhigalovo meteorology station (55 km south of Botovskaya) are recorded by the navy blue line (Klein Tank et al., 2002).